Supplemental material

New shuttle vectors for gene cloning and expression in multidrug-resistant *Acinetobacter* species

by Massimiliano Lucidi, Federica Runci, Giordano Rampioni, Emanuela Frangipani, Livia Leoni and Paolo Visca

Including figures S1, S2, S3, S4, S5, S6, S7 and tables S1 and S2

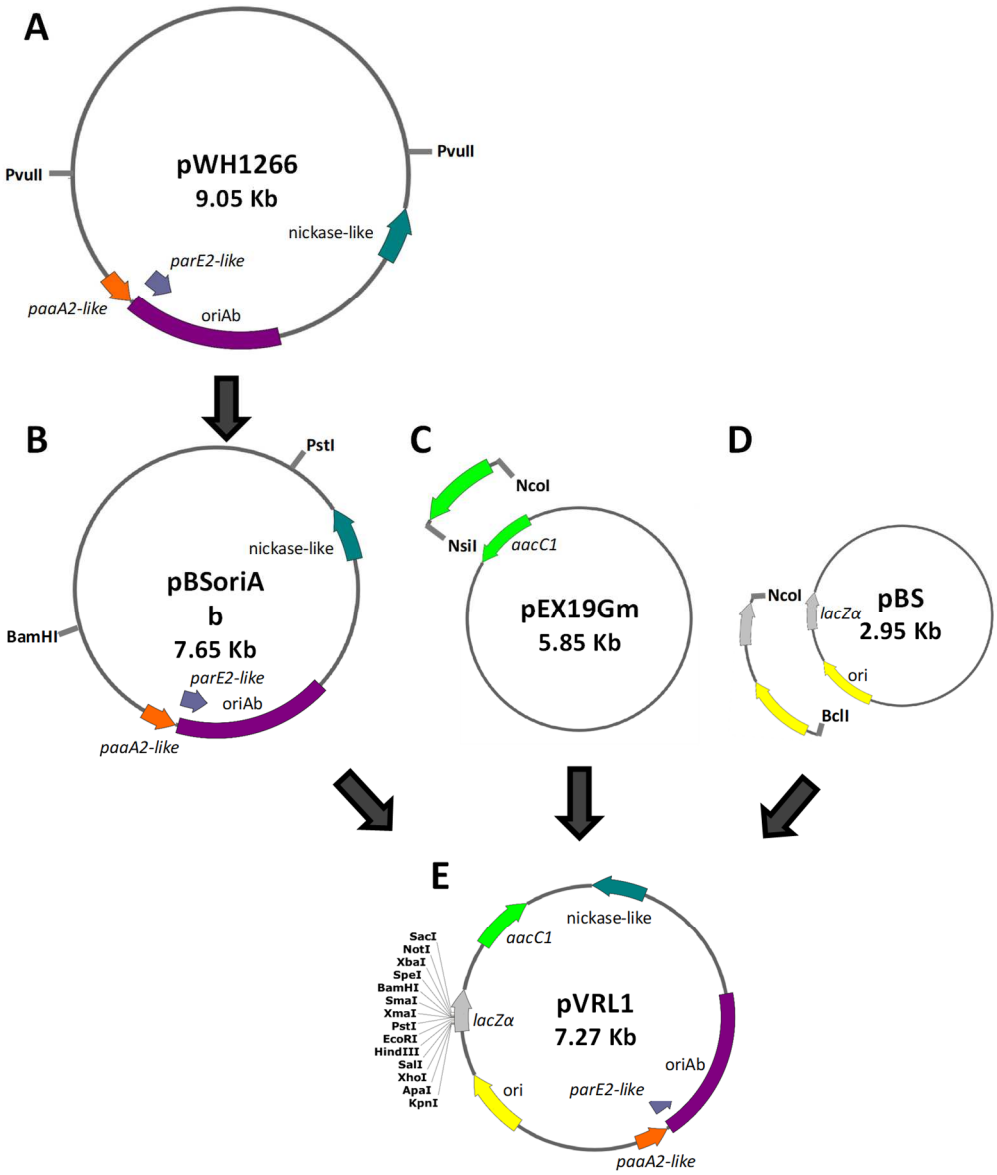

FIG S1 Schematic representation of cloning steps in pVRL1 construction. (A) pWH1266 was digested at PvuII restriction sites to obtain the 4,693-bp replication and maintenance region for *A. baumannii.* This region contains the oriAb (violet), *paaA2*-like antitoxin gene (orange), *parE2*-like toxin gene (light purple) and the *nickase*-like gene (cyan). The 4,693-bp fragment was then cloned into the SmaI site of pBS, to obtain pBSoriAb (B). The Gm-resistance cassette (green) was amplified by PCR from pEX19Gm (C), while the ColE1-like origin of replication (yellow) and the MCS within the *lacZ*α gene (grey), were amplified by PCR from pBS (D). Amplicons with artificially-introduced restriction sites (Table S1) are shown as external arcs of circle. The oriAb fragment was obtained from pBSoriAb by digestion with BamHI and PstI, while the amplicons derived from pBS and pEX19Gm were digested with BclI/NcoI and NcoI/NsiI, respectively. All the three DNA digestion products were directionally ligated to obtain the pVRL1 vector (E), since BclI-BamHI and NsiI-PstI generate compatible cohesive ends. The relevant features of each plasmid are indicated with colours. Unique cutter restriction enzymes are highlighted in bold. All genes are reported in scale over the total length of the vector. Image obtained by Snapgene software (from GSL Biotech; available at snapgene.com).

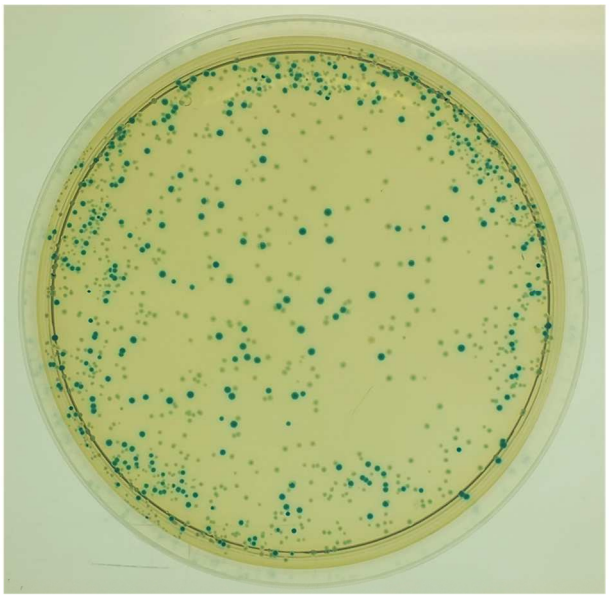

FIG S2 Blue/white screening for the detection in *E. coli* DH5α carrying the $trpE_{wt}$ gene in pVRL1. The $trpE_{wt}$ gene was amplified from *A. baumannii* ATCC19606^{T} genome and then cloned into the MCS of the pVRL1 plasmid. All white colonies screened contained the $trpE_{wt}$ gene, whereas blue colonies did not. Clones were screened with both PCR and analytic digestion (data not shown).

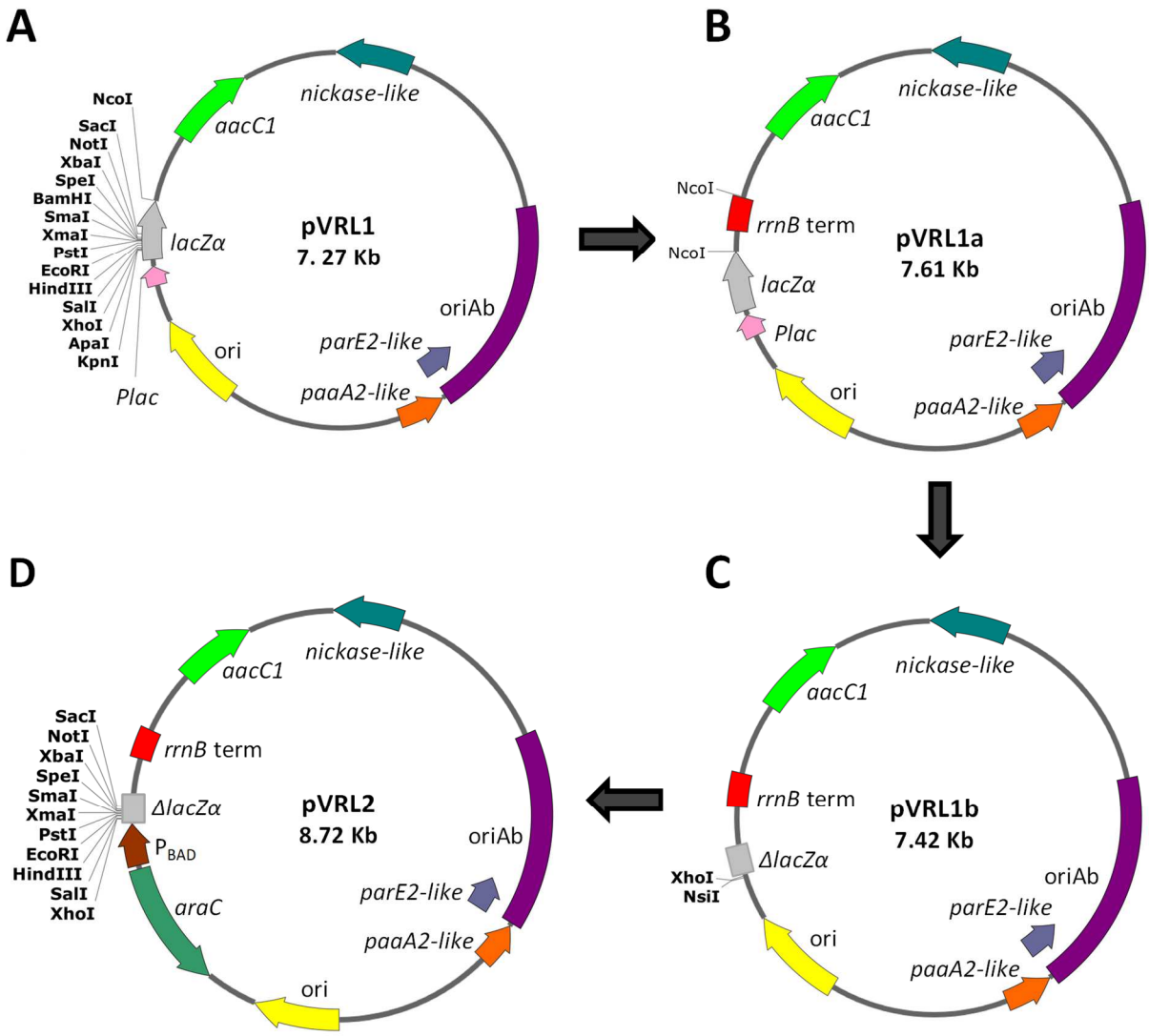

FIG S3 Schematic representation of cloning steps in pVRL2 construction. pVRL1 (A) was digested at the unique NcoI restriction site, to insert the *rrnB* transcriptional terminators (*rrnB* term; red box) to obtain pVRL1a (B). The region including the pVRL1a *lac* promoter (*Plac*, pink), CAP binding site and the first 24 codons of the *lacZα* ORF (Δ*lacZα*; gray) were deleted to obtain pVRL1b (C). An arabinose inducible regulatory element, composed of the *araC* gene and the P_{BAD} promoter (indicated in dark green and brown, respectively) was introduced in pVRL1b, to obtain the expression plasmid pVRL2 (D). Relevant features of plasmids are in indicated with different colours: Gm-resistance cassette (green); *nickase*-like gene (cyan); *paaA2*-like antitoxin gene (orange); *parE2*-like toxin gene (light purple); ColE1-like origin of replication (yellow); and oriAb (violet). Unique cutter restrictions enzymes are in bold. All the genes are reported in scale over the total length of the vector. Image obtained by the Snapgene software (from GSL Biotech; available at snapgene.com).

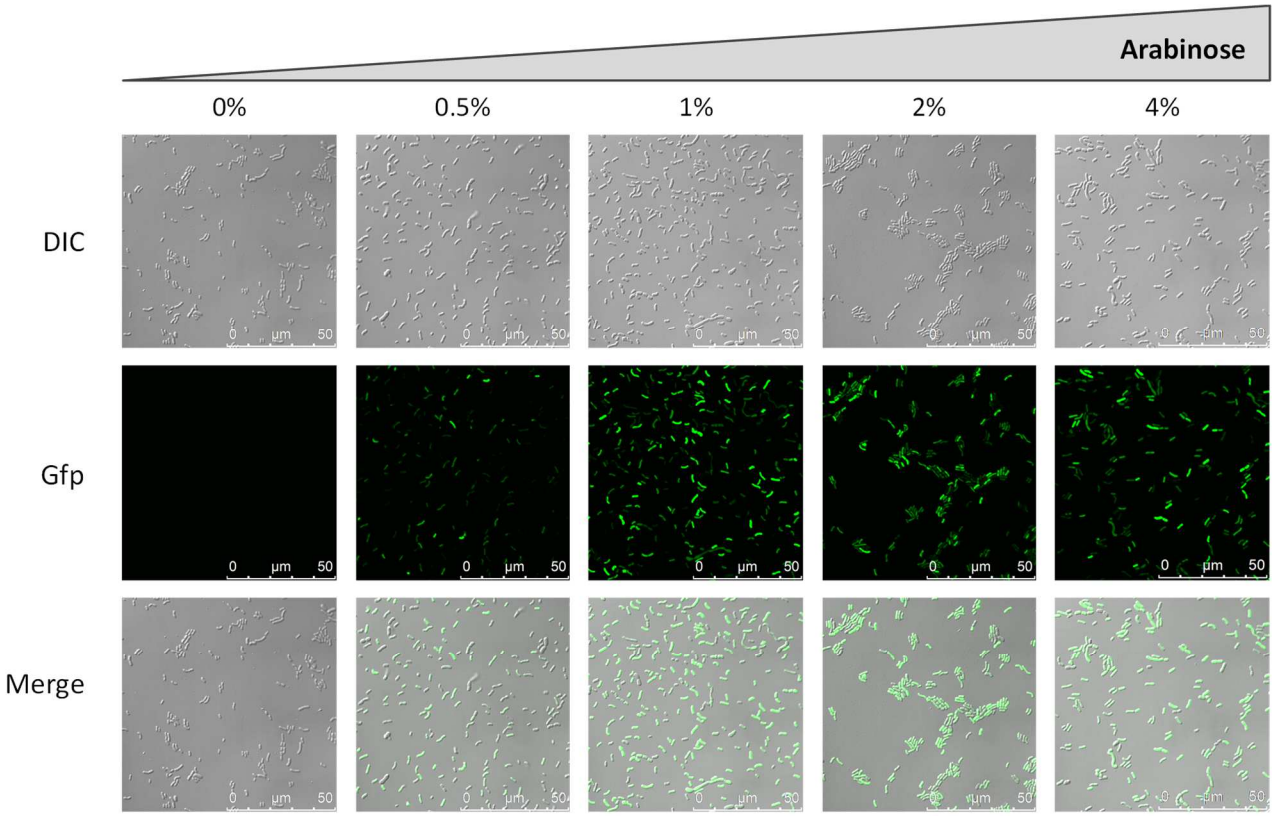

FIG S4 Arabinose inducible expression of the *gfp* gene under the control of the *araC*-P_{BAD} promoter in plasmid pVRL2*gfp*. Expression of the fluorescent protein Gfp was investigated using confocal microscopy. Six hours after addition of arabinose, *A. baumannii* ATCC19606^T cells carrying pVRL2*gfp* were observed by confocal microscopy. The fluorescence emission upon excitation at 475 nm was used to assess the presence of cell-associated fluorescence (Gfp). Representative images are shown. A Leica SP5 confocal laser scanning microscope equipped with a 63× oil immersion objective was used. Scale bar, 50 µm. DIC, differential interference contrast; Merge, merged DIC and Gfp images.

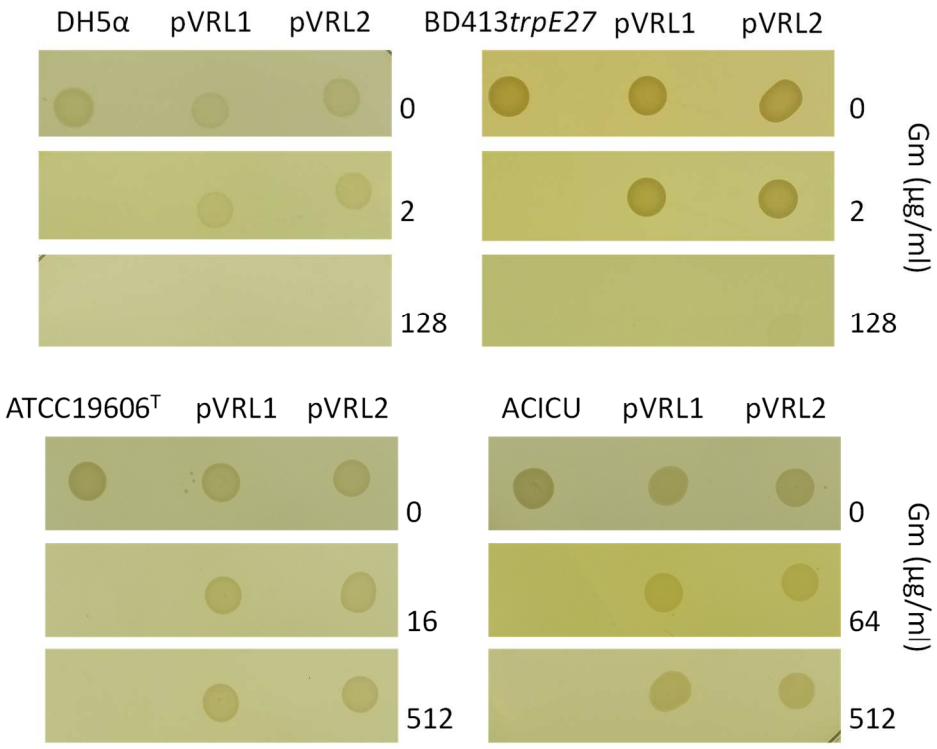

FIG S5 Minimum Inhibitory Concentration (MIC) of gentamicin on LA for strains carrying the pVRL plasmids. Bacterial suspensions containing *ca*. 5 × 10^4 CFU were spotted on LA containing different gentamicin (Gm) concentrations (0 to 512 µg/ml). The MICs, when available, were determined after 24 hours of incubation at 37°C.

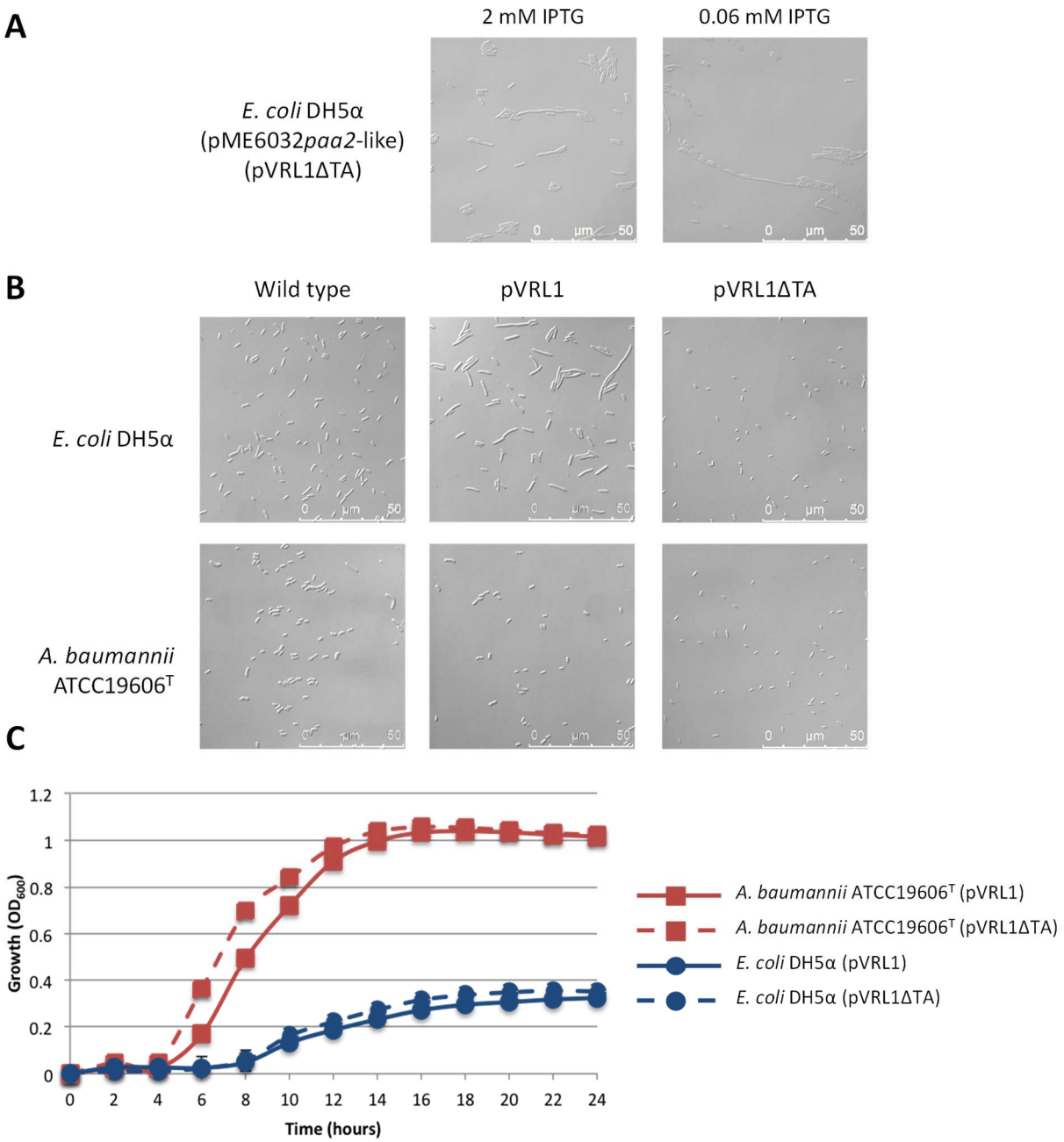

FIG S6 The presence of a toxin-antitoxin (TA) system affects *E. coli* cell morphology without disturbing bacterial growth. (A) Morphology of *E. coli* DH5α harbouring both pVRL1Δ*paaA2*-like and pME6032*paaA2*-like plasmids, grown in the presence of IPTG (2 and 0.06 mM), as observed by confocal microscopy. (B) *E. coli* DH5α and *A. baumannii* ATCC19606^T cells were observed using confocal microscopy. *E. coli* DH5α cells harbouring pVRL1 showed a filamentous shape, while deletion of TA system (pVRL1ΔTA) restored the normal morphology. No effect on morphology was observed for *A. baumannii* ATCC19606^T, independently of plasmid carriage. Wild type strains were used as controls. Scale bar: 50 µm. (C) Growth of *E. coli* DH5α and *A. baumannii* ATCC19606^T harbouring pVRL1 or pVRL1ΔTA in LB supplemented with Gm (10 µg/ml for *E. coli* and 100 µg/ml for *A. baumannii*). Data are the mean ± SD of three independent experiments.

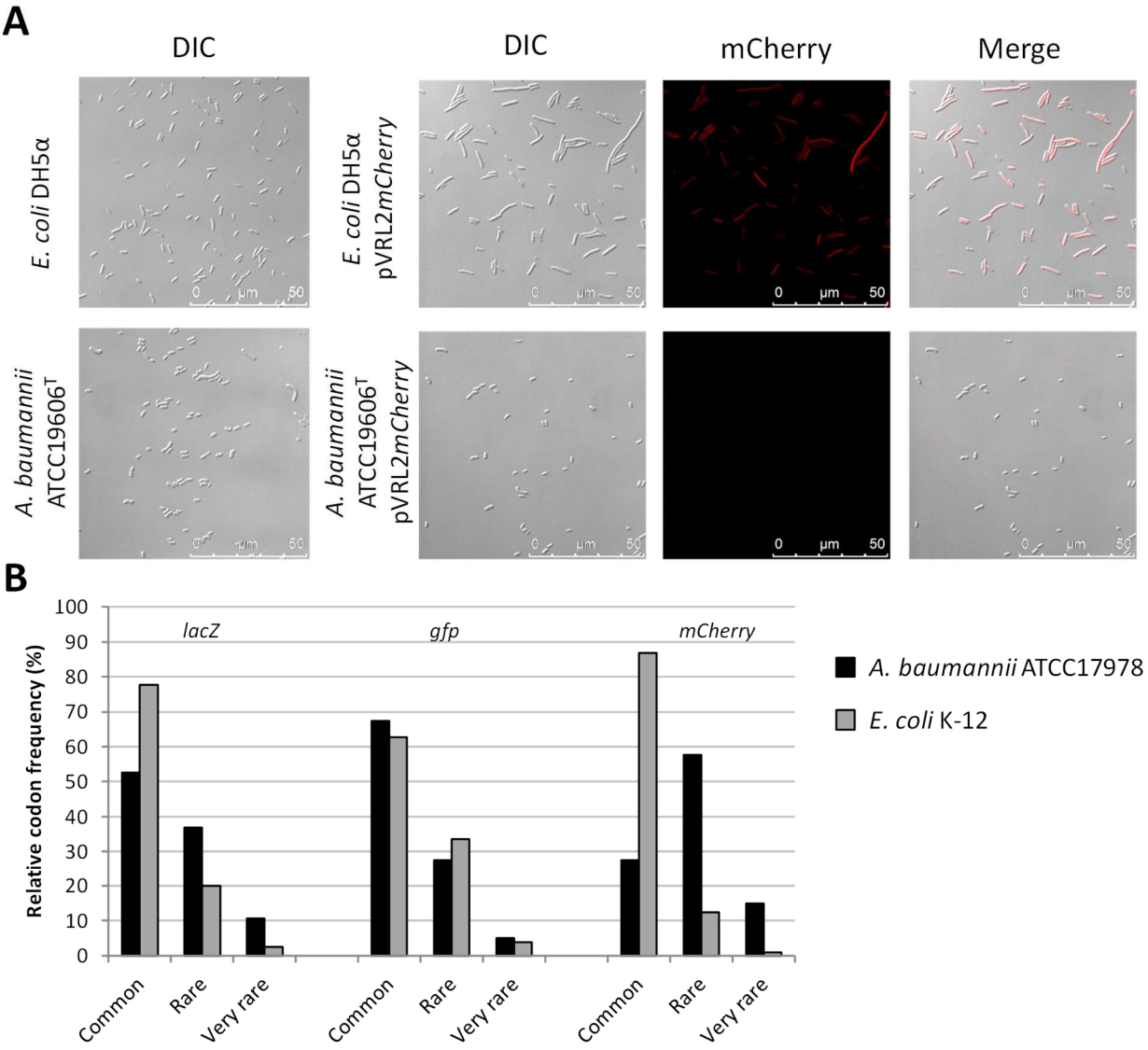

FIG S7 The codon usage affects the arabinose inducible expression of the genes cloned in pVRL2. (A) The presence of the fluorescent protein mCherry expressed by *E. coli* DH5α and *A. baumannii* ATCC19606^T carrying pVRL2*mCherry*, was detected by confocal microscopy of bacterial cultures grown in the presence of 1% arabinose. The fluorescence emission upon excitation at 587 nm was used to assess the presence of cell-associated fluorescence (mCherry). Scale bar, 50 µm. DIC, differential interference contrast; Merge, merged DIC and mCherry images. (B) Relative codon frequency in *lacZ*, *gfp* and *mCherry* sequences determined for *A. baumannii* ATCC17978 (dark bars) and *E. coli* K-12 (grey bars) using Graphical Codon Usage Analyser (http://gcua.schoedl.de/). Different thresholds for codon usage are indicated: common (>25%), rare (10 to 25%) and very rare (<10%).

Table S1. Primers

Primer	Restriction site	Sequence (5'-3')[a]	Use
MCS ori ColE1-like FW	NcoI	**CATG**CCATGGTTACAATTTCCATTCGCCATT	Amplification of ColE1-like origin, MCS and *lacZα* from pBS; Sequencing of pVRL1
MCS ori ColE1-like RV	BclI	**CTG**TGATCACAAGTTTACTCATATATACTTTA	Amplification of ColE1-like origin, MCS and *lacZα* from pBS; Sequencing of pVRL1
aacC1 FW	NcoI	**CTAC**CCATGGTCGTGATACGCCTATTTTTAT	Amplification of gentamicin resistance cassette from pEX19Gm; Sequencing of pVRL1
aacC1 RV	NsiI	**CCA**ATGCATACTTGGTCTGACAATCGATG	Amplification of gentamicin resistance cassette from pEX19Gm; Sequencing of pVRL1
oriAb FW1	-	CAATGAGTAGTCATTTAATTGGC	Sequencing of pWH1277-derived portion of pWH1266 and pVRL1
oriAb FW2	-	GATCGTAGAAATATCTATGATT	Sequencing of pWH1277-derived portion of pWH1266 and pVRL1
oriAb RV	-	GGATTTTAACATTTTGCGTTG	Sequencing of pWH1277-derived portion of pWH1266 and pVRL1
Seq. 1a	-	GAGTTGTTCGGTAAATTGTCA	Sequencing of pWH1277-derived portion of pWH1266 and pVRL1
Seq. 1b	-	CTAGCCCTTGCGGTGTAAGG	Sequencing of pWH1277-derived portion of pWH1266 and pVRL1
Seq. 2	-	TAGATCCTTTTAAATTAAAAATGAA	Sequencing of pVRL1
Seq. 3a	-	TAATCGCTTCCTATGACGTT	Sequencing of pWH1277-derived portion of pWH1266 and pVRL1
Seq. 3b	-	TAAGCGGCTGTATGCAGTG	Sequencing of

			pWH1277-derived portion of pWH1266 and pVRL1
Seq. 4	-	AATCATCAATTTCAATAGCTGC	Sequencing of pWH1277-derived portion of pWH1266 and pVRL1
Seq. 5	-	GTTTAATTATTCTTACTAATATTATCT	Sequencing of pWH1277-derived portion of pWH1266 and pVRL1
Seq. 6	-	GTTGGGAGTAGGTGGCTAC	Sequencing of pVRL1
Seq. 7	-	GGTTTGCGTATTGGGCGCTC	Sequencing of pVRL1
Seq. 8	-	CGGCTATGTCAAAGATGCTG	Sequencing of pWH1277- derived portion of pWH1266 and pVRL1
Seq. 9	-	CAGCCTGTTGCATCTGCTCAT	Sequencing of pWH1277- derived portion of pWH1266 and pVRL1; Verification of correct orientation of *rrnB* terminators
Seq. 10	-	GGTATCTGCGCTCTGCTG	Sequencing of pVRL1
Seq. 11	-	CATTCATCGCGCTTGCTGCC	Sequencing of pVRL1
Seq. 12	-	GACCACTCCTGCGATGTGTG	Sequencing of pWH1277- derived portion of pWH1266 and pVRL1
*rrnB*term FW	NcoI	**CATG**CCATGGTGCCTGGCGGCAGTAGCG	Amplification of *rrnB* terminators from pEX19Gm
*rrnB*term RV	NcoI	**CATG**CCATGGAAACGCAAAAAGGCCATCCG	Amplification of *rrnB* terminators from pEX19Gm; Verification of correct orientation of *rrnB* terminators
Δ*lac*P FW	XhoI	**CGC**CTCGAGGTCAACGGTATC	Primer flanking *lac* promoter in pVRL1a used for deletion
Δ*lac*P RV	NsiI	**CCA**ATGCATCTTTCCAGTCGGGAAACC	Primer flanking CAP binding site in pVRL1a used for deletion

araC P_{BAD} FW	NsiI	**CCA**ATGCATAATGTGCCTGTCAAAT	Amplification of *araC* and P_{BAD} from miniCTX1-*araC*-P_{BAD}-*tolB* and cloning in pVRL1b
araC P_{BAD} RV	XhoI	**CCG**CTCGAGATTCAGAAGGTTAGCCCAAAA	Amplification of *araC* and P_{BAD} from miniCTX1-*araC*-P_{BAD}-*tolB* and cloning in pVRL1b
trpE prom.	XhoI	**CCG**CTCGAGTATCTGCTTCACAATCATTAATGA	Amplification of *trpE* gene with its endogenous promoter
trpE ATG FW	XhoI	**CCG**CTCGAGATGACTACATTAGCGCAATTCG	Amplification of *trpE* gene
trpE RV	PstI	**AAAA**CTGCAGTCATAAAATCAATCCGTTTGATG	Amplification of *trpE* gene
lacZ FW	XhoI	**CCG**CTCGAGATGACCATGATTACGGATTCAC	Amplification of *lacZ* gene
lacZ RV	PstI	**AAAA**CTGCAGTTATTTTTGACACCAGACCAACT	Amplification of *lacZ* gene
tetA FW	XhoI	**CCG**CTCGAGATGAAATCTAACAATGCGCTCA	Amplification of *tetA* gene
tetA RV	PstI	**AAAA**CTGCAGGAGGTGCCGCCGGCTTC	Amplification of *tetA* gene
mCherry FW	XhoI	**CCT**CTCGAGGTGAGCAAGGGCGAGGAG	Amplification of *mCherry* gene
mCherry RV	EcoRI	**CCG**GAATTCTCACTTGTACAGCTCGTCC	Amplification of *mCherry* gene
Zeo1 FW	NsiI	**CCA**ATGCATTTCTCCTTACGCATCTGTGC	Amplification of zeocin resistance cassette from pCR™-Blunt II-TOPO®
Zeo1 RV	NsiI	**CCA**ATGCATGTGTCAGTCCTGCTCCTCG	Amplification of zeocin resistance cassette from pCR™-Blunt II-TOPO®
Zeo2 FW	KpnI	**GGT**GGTACCTTTCTCCTTACGCATCTGTGC	Amplification of zeocin resistance cassette from pCR™-Blunt II-TOPO®
Zeo2 Rv	ApaI	**ACC**GGGCCCGTGTCAGTCCTGCTCCTC	Amplification of zeocin resistance cassette from pCR™-Blunt II-TOPO®

pVRL1Δ*aacC1* FW	NsiI	**CCT**ATGCATCTACTTGCATTACAGTTTACGAAC	Primer flanking *aacC1* gene in pVRL1 used for deletion of Gm resistance cassette
pVRL1Δ*aacC1* RV	NsiI	**CCA**ATGCATACCAAGTATGCAGCCCCT	Primer flanking *aacC1* gene in pVRL1 used for deletion of Gm resistance cassette
pVRL2Δ*aacC1* FW	KpnI	**CCG**GGTACCCTACTTGCATTACAGTTTACGAAC	Primer flanking *aacC1* gene in pVRL2 used for deletion of Gm resistance cassette
pVRL2Δ*aacC1* RV	ApaI	**ACC**GGGCCCACCAAGTATGCAGCCCCT	Primer flanking *aacC1* gene in pVRL2 used for deletion of Gm resistance cassette
ΔTA FW	-	CTTACTCATGTACTTTGGATTATTTAG	Primer flanking TA system in pVRL1 used for deletion (generation of pVRL1ΔTA)
ΔTA RV	BclI	**CTC**TGATCAGTTTTTCACTCCAATGTGTTAC	Primer flanking the antitoxin gene *paaA2*-like system in pVRL1 used for the deletion of the TA system (generation of pVRL1ΔTA) and the deletion of *paaA2*-like gene (generation of pVRL1ΔpaaA2-like)
Δ*paaA2*-like FW	-	ATGAAGATTGAGTGGACTG	Primer flanking the antitoxin *paaA2*-like gene in pVRL1 used for the deletion of *paaA2*-like gene (generation of pVRL1ΔpaaA2-like)
paaA2-like FW	EcoRI	**CCG**GAATTCATGACAGAAGCGACTTTTAC	Amplification of *paaA2-like* antitoxin gene
paaA2-like RV	SacI	**ACC**GAGCTCTCCACTCAATCTTCATTCTTCG	Amplification of *paaA2-like* antitoxin gene
aacC1 PCN FW	-	GATCTATATCTATGATCTCGC	Determination of pVRL1 copy number in *E. coli* and *A. baumannii*

aacC1 PCN RV	-	GATCACATAAGCACCAAGCG	Determination of pVRL1 copy number in *E. coli* and *A. baumannii*
dxs Ab FW	-	AGTTTGGGATGTGGGACACC	Determination of pVRL1 copy number in *A. baumannii*. Amplification from nt 195,274 to nt 195,387 encompassing an internal fragment (113 bp) of gene HMPREF0010_01955
dxs Ab RV	-	CTTCTCTGGCTGGGAAAGCA	Determination of pVRL1 copy number in *A. baumannii*. Amplification from nt 195,274 to nt 195,387 encompassing an internal fragment (113 bp) of gene HMPREF0010_01955
dxs Ec FW	-	CGAGAAACTGGCGATCCTTA	Determination of pVRL1 copy number in *E. coli*. Amplification from nt 436,807 to nt 436,694 encompassing an internal fragment (113 bp) of gene G6237
dxs Ec RV	-	CTTCATCAAGCGGTTTCACA	Determination of pVRL1 copy number in *E. coli*. Amplification from nt 436,807 to nt 436,694 encompassing an internal fragment (113 bp) of gene G6237

[a] GC clamps are shown in bold; restriction sites are underlined.

Table S2. Comparison of I-TASSER and SWISS-MODEL prediction scores for the ParE2-PaaA2-like toxin-antitoxin system of pWH1277

Predicted protein (ORF)	Accession number of proteins predicted by BLASTX analyses	I-TASSER template (PDB ID; reference)	TM-score[a]	SWISS-MODEL template (PDB ID; reference)	QMEAN[b]
Putative toxin (ORF-3)	WP005166293.1	*E. coli* ParE2 toxin (5CW7; ref. 1)	0.969	*E. coli* ParE2 toxin (5CW7; ref. 1)	-1.48
Putative antitoxin (ORF-2)	WP005166297.1	*E. coli* YafQ antitoxin (4ML0; ref. 2)	0.571	*E. coli* YafQ antitoxin (4Q2U; ref. 3)	-2.43

[a] TM-score is a measure of global structural similarity between query and template protein; the value is comprised between 0 (lowest similarity) and 1 (highest similarity);
[b] The global and per-residue model quality has been assessed using the QMEAN scoring function (4).

Supplementary references

1. Sterckx YG, Jove T, Shkumatov AV, Garcia-Pino A, Geerts L, De Kerpel M, Lah J, De Greve H, Van Melderen L, Loris, R. 2016. A unique hetero-hexadecameric architecture displayed by the *Escherichia coli* O157 PaaA2-ParE2 antitoxin-toxin complex. J Mol Biol. 428: 1589-1603.
2. Liang Y, Gao Z, Wang F, Zhang Y, Dong Y, Liu Q. 2014. Structural and functional characterization of *Escherichia coli* toxin-antitoxin complex Dinj-Yafq. *J Biol Chem* 289:21191-21202.
3. Ruangprasert A, Maehigashi T, Miles SJ, Giridharan N, Liu JX, Dunham CM. 2014. Mechanisms of toxin inhibition and transcriptional repression by *Escherichia coli* DinJ-YafQ. J Biol Chem 289:20559-20569.
4. Benkert P, Biasini M, Schwede T. 2011. Toward the estimation of the absolute quality of individual protein structure models. Bioinformatics 27:343-350.